atmosphere

MDPI

Article

Ozone Variation during the Development of a Tropical Cyclone: Case Study

Saleha Al-Kallas [1], Motirh Al-Mutairi [1], Heshmat Abdel Basset [2], Ayman Badawy [3], Abdallah Abdeldym [2,*] and Mostafa Morsy [2]

[1] Faculty of Arts, Princess Nourah Bint Abdulrahman University, Riyadh 11671, Saudi Arabia; sahalkallas@pnu.edu.sa (S.A.-K.); dr.motirh@hotmail.com (M.A.-M.)
[2] Department of Astronomy and Meteorology, Faculty of Science, Al-Azhar University, Cairo 11651, Egypt; heshmatm@yahoo.com (H.A.B.); mostafa_morsy@azhar.edu.eg (M.M.)
[3] Egyptian Meteorological Authority, Cairo 11784, Egypt; mnbadawe4@gmail.com
* Correspondence: abdallh905@azhar.edu.eg; Tel.: +20-102-662-3397

Abstract: The aim of this work was to study the variation in the total ozone column amount (TOC) during the life cycle of the tropical cyclone (TC) that occurred over the northwest Indian Ocean from 14 to 25 October 2008. This goal was achieved through examining the behavior of the tropical cyclone tilt under vertically varying background flows in association with the cyclone development. Thus, the vertical wind shear (VWS) was estimated as one of the most important dynamical parameters related to TC formation and intensity changes. Moreover, we estimated the variations in the daily values of TOC during the period of cyclone activity. We found that the magnitude of VWS increased during the growth period, and VWS weakened during the decay period. Anomalies of daily TOC were found to reduce steadily before and during the cyclone formation, followed by an increasing trend after the dissipation of cyclone. It was also found that during the development of the tropical cyclone, an outflow developed in the upper levels, having high velocities that extended beyond the tropopause up to the lower stratosphere. As a result, the lowest value of TOC during the tropical cyclone was due to a large amount of injected water vapor from the troposphere into the stratosphere through the convection processes. This was mostly photo-dissociated into OH and atomic O by deep solar radiation in the upper and lower stratosphere, leading to a severe reduction in stratospheric ozone.

Keywords: total ozone column; tropical cyclone; tilt; vertical wind shear; cyclogenesis; stratosphere-troposphere exchange; ozone mixing ratio

Citation: Al-Kallas, S.; Al-Mutairi, M.; Basset, H.A.; Badawy, A.; Abdeldym, A.; Morsy, M. Ozone Variation during the Development of a Tropical Cyclone: Case Study. *Atmosphere* **2021**, *12*, 1582. https://doi.org/10.3390/atmos12121582

Academic Editor: Alexandru Rap

Received: 14 November 2021
Accepted: 22 November 2021
Published: 27 November 2021

1. Introduction

Tropical cyclones play an important role in the stratosphere–troposphere exchange (upward and downward transport) through their associated deep convection [1,2]. Stratospheric intrusions carry the ozone-rich air from the stratosphere into the troposphere [3–5], whereas the boundary layer ozone-poor air rises to the upper troposphere and lower stratosphere (UTLS) regions [6–10]. Many studies have examined the relationship between tropical cyclones (TCs) and TOC; for example, Baray et al. [1] detailed the stratosphere–troposphere exchange (STE) during Cyclone Marlene and noted a maximum change in ozone at the 300 hPa level. In a study of the perturbation in the TOC due to four severe TCs occurring over the Arabian Sea and the Bay of Bengal, Singh and Nair [11] found that, at the maximum strength of cyclones, the negative anomalies (>20 Dobson) occurred in the daily TOC. Midya et al. [12] also identified a steady reduction in TOC before and during the cyclone development, whereas after the decay of the cyclone, an approximately cumulative trend was noticed. Tropical cyclones often develop with considerable shifts between the centers of the circulation at the surface and the upper level. The direction of these shifts in the centers of circulation (slope or tilt) is in the direction of the convective cloud mass, which in the first stage of formation moves from the surface centers, whereas

this slope decreases to become aligned vertically when the cyclone intensifies. The TC's structure and strength are significantly affected by the vertical wind shear (VWS). In the inner core the moderate-to-strong shear tends to create convective asymmetries, with the prevailing maximum convection in the downward and shear-left direction of the wind shear vector [13–19]. The balanced response of the vortex tilt, which causes the upward airflow to tilt downward, is used to account and explain for the existence of such an asymmetry. The general objective of the current work was to study the variation in TOC during the activity period of the tropical cyclone that appeared above the Indian Ocean during the period from 14 to 25 October 2008. The study was planned as follows: first, we chose the example of the tropical cyclone and studied its synoptic condition; second, we examined its development through the slope of the line connecting the center of the cyclone at different levels (vertical axis tilt) by estimating the wind shear between the levels 1000 and 100 hPa during the cyclone's life cycle. In the third step, we examined the variation in TOC during the activity of the tropical cyclone.

2. Data and Statistical Procedures

Data Acquisition

The meteorological data used to achieve the purposes of this study were obtained from the European Centre for Medium-Range Weather Forecasts (ECMWF) ERA-Interim reanalysis dataset [20] with spatial resolution 1° × 1° every 6 h (00Z, 06Z, 12Z and 18Z) during the tropical cyclone from 14 to 25 October 2008. The total column ozone (TCO, DU), mean sea level pressure (P, hPa) and near surface temperature (T, °C) were downloaded from https://apps.ecmwf.int/datasets/data/interim-full-daily/levtype=sfc/ (accessed on 22 November 2021). The extracted meteorological parameters at 37 isobaric levels (1–1000 hPa) were temperature (T, °C), zonal and meridional wind components (u and v, m/s), relative humidity (RH, %), geopotential height (H, gpm), vertical motion (ω, Pa/s) and ozone mass mixing ratio (OMR, PPM), which were downloaded from https://apps.ecmwf.int/datasets/data/interim-full-daily/levtype=pl (accessed on 22 November 2021). The extracted domain of study extended from 10° S to 40° N and 30° E to 95° E (Figure 1).

In the present study, two domains were used: the first mother domain was used for the synoptic and spatial distribution of TOC, VWS, and RH analysis and extended latitudinally from 0 to 30° N and longitudinally from 25° E to 85° E, whereas the inner domain was used for calculation of the TOC, OMR, RH, and ω variations and its position changes with time to represent our cyclone throughout its life cycle (Figure 2). For each day, average TOC was estimated by calculating the average gridded ozone values inside the domain of calculations (Figure 2). This domain encloses the cyclone cell throughout the study, and so, our calculations of TOC average and meteorological parameters were made only over our domain to enable a better view and investigation of the total amount of ozone variation with meteorological parameters. The vertical wind shear (VWS) between the different two pressure levels is calculated as follows:

$$\text{VWS L1-L2} = |\text{V L1} - \text{V L2}|$$

where V is the value of the area average of horizontal wind specified either within the mother domain or over the inner domain of calculation (Figure 2), and L1 and L2 represent distinct two pressure levels. We initially investigated the sensitivity to the bottom pressure level by changing lev2 from 1000 to 500 hPa and discovered that the bottom pressure level at 1000 hPa has the strongest correlation between TC intensity change and VWS. Our calculations show that the VWS between 100 and 1000 hPa is more representative of the attenuating deep-layer shear effect than the commonly used VWS measure between 200 and 850 hPa.

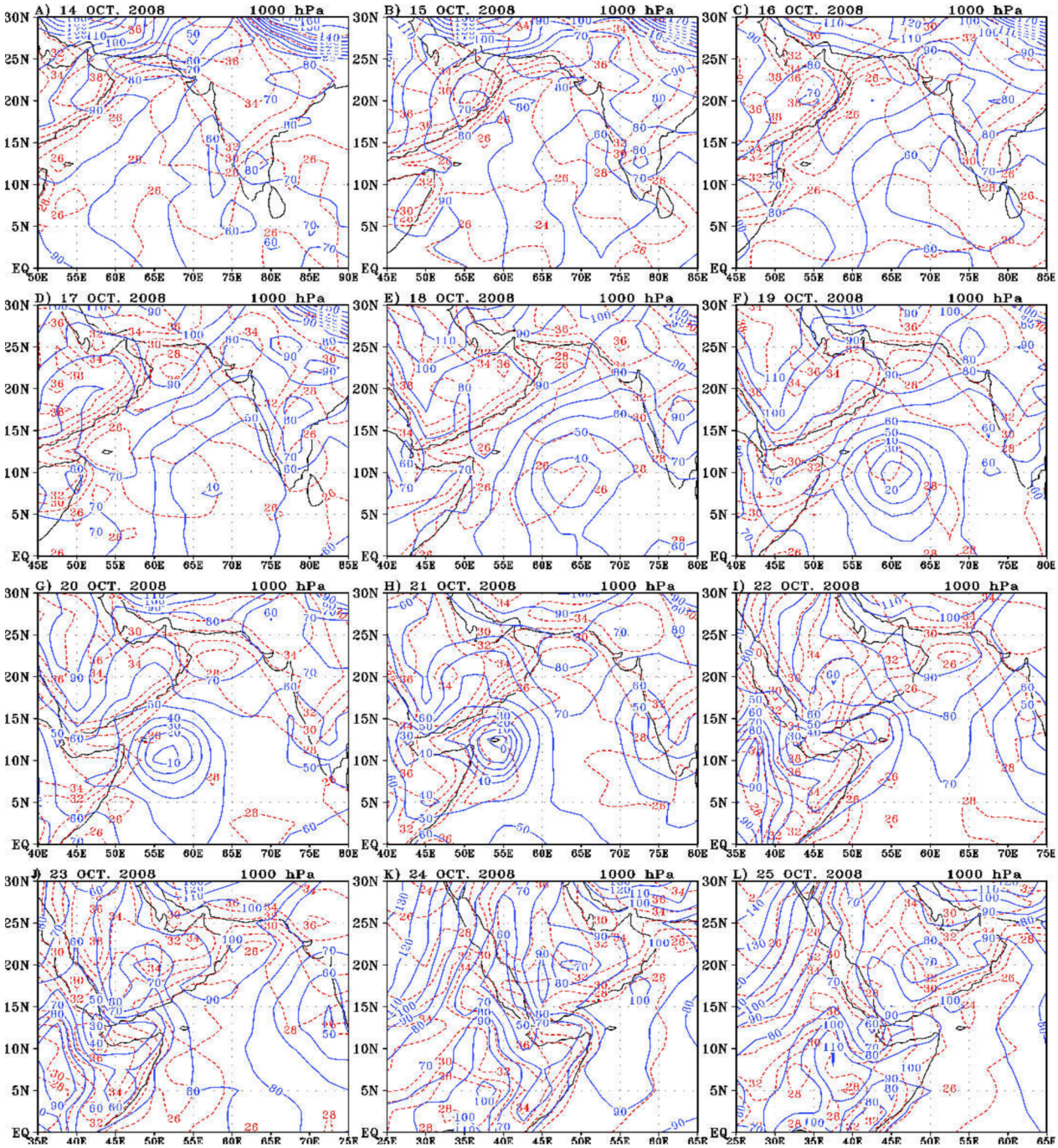

Figure 1. Height contours of 1000 hPa in 10 gpm intervals (blue solid lines) and temperature (red dashed lines) in 2 °C increments at 12Z for 14–25 October 2008 (**A**–**L**).

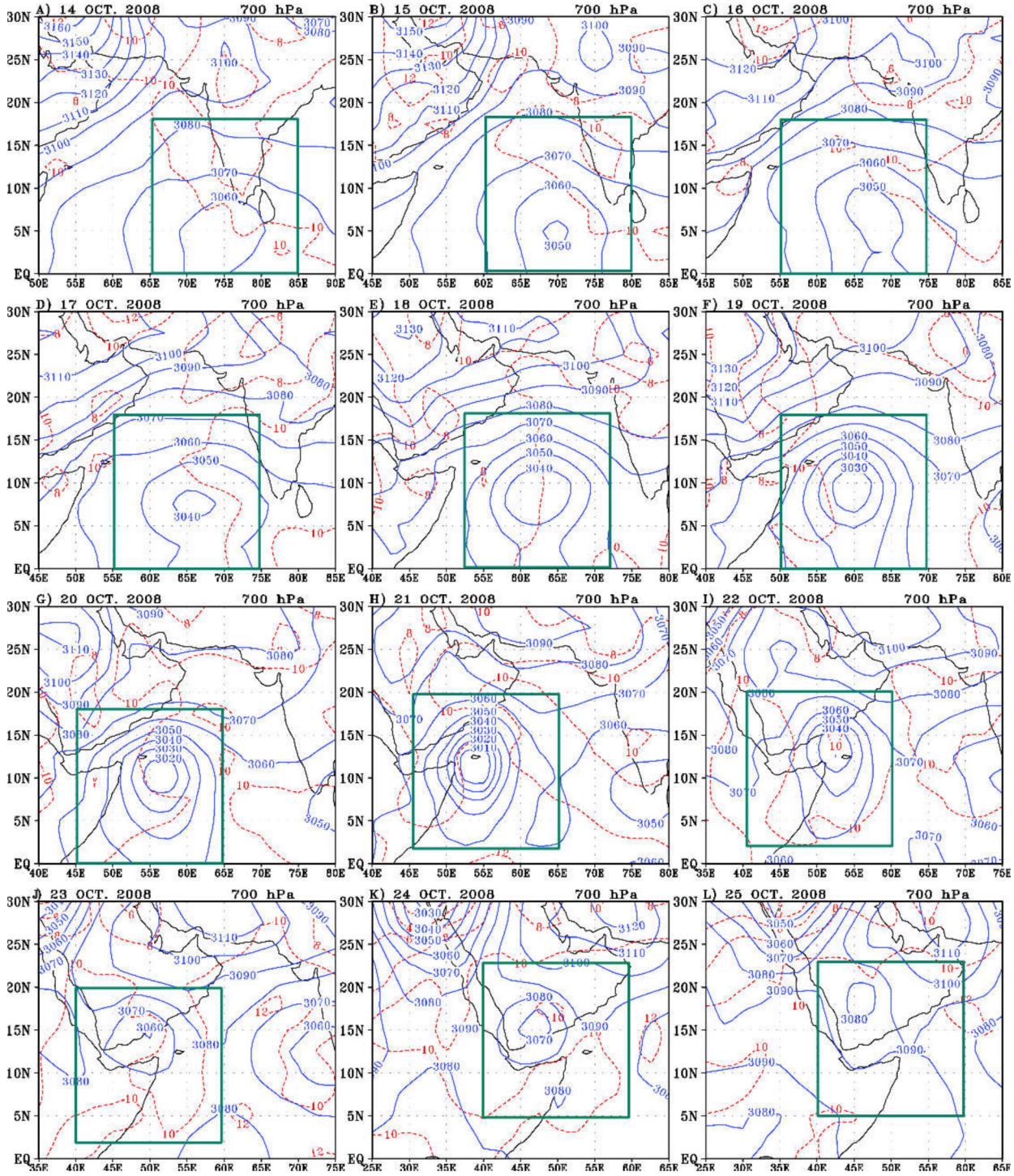

Figure 2. Height contours of 700 hPa in 10 m intervals (blue solid lines) and temperature (red dashed lines) in 2 °C increments at 12Z for 14–25 October 2008 (**A**–**L**).

3. Results and Discussions

3.1. Synoptic Discussion

A tropical cyclone occurred above the Indian Ocean during the period from 14 to 25 October 2008. Figures 1 and 2 show the horizontal distribution of the geopotential height with 10 gpm contour intervals and temperature isotherms every 2 °C on 1000 and 700 hPa at 12Z during the period from 14 to 25 October. The synoptic pattern of the depression was followed to determine its track, in addition to the value of pressure and temperature at its center for each day from 14 to 25 October. Figure 3a shows the track

of the tropical depression during the period from 14 to 25 October 2008, and Figure 3b illustrates the temperature and pressure values at the center of the TC through the period of study. According to the variations in pressure and temperature in the cyclone center at the surface (Figure 3a,b), and the development and movement of the cyclone on 1000 and 700 hPa (Figures 1 and 2), we can divide the life cycle of the cyclone into three periods: the first period is the pre-storm period, which extended from 14 to 16 October; the second period (growth period) is from 17 to 21 October; and the third period (decay period) is from 22 to 25 October.

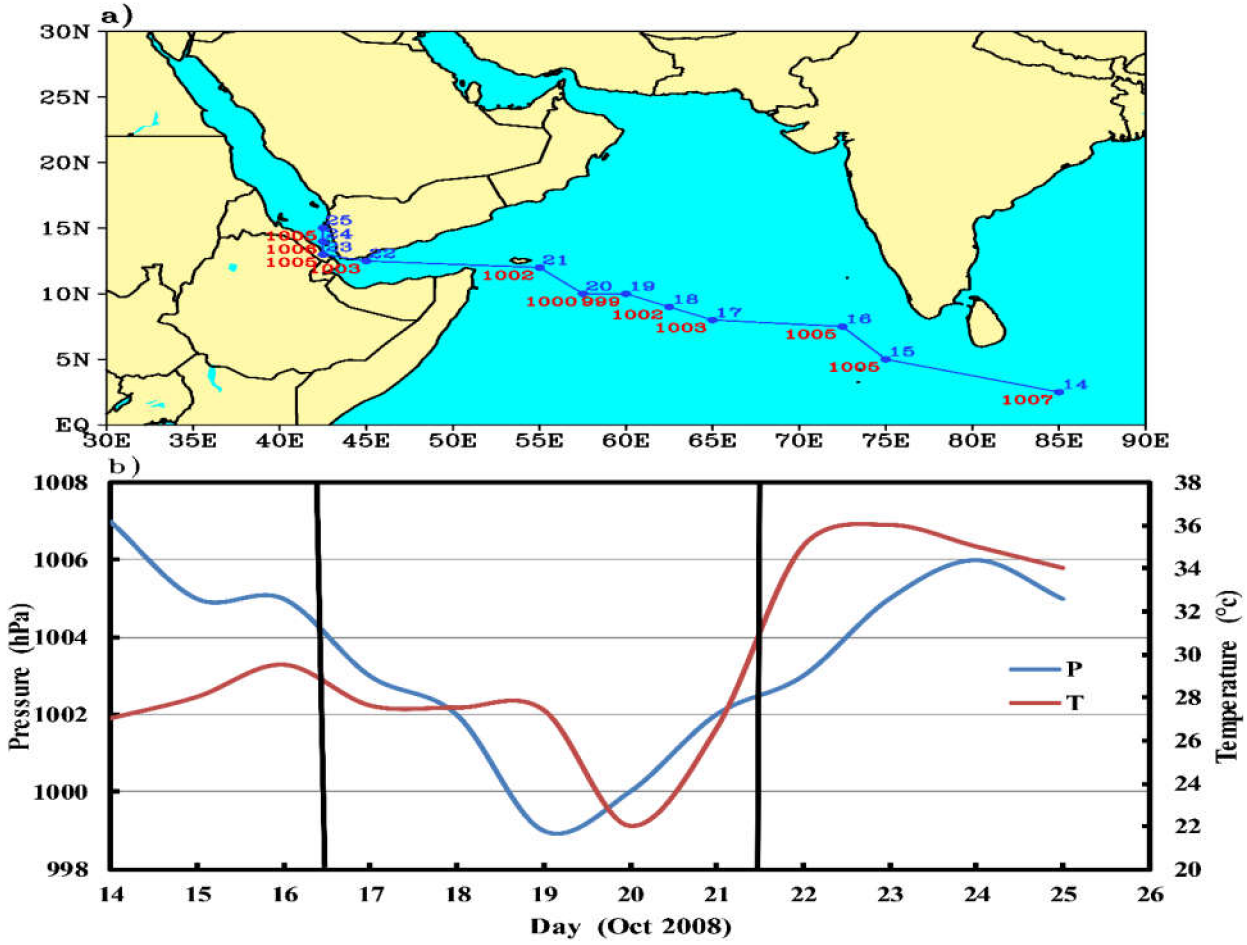

Figure 3. (**a**) The track of the tropical cyclone during the period from 14 to 25 October 2008. (**b**) The values of pressure and temperature at the center of the tropical cyclone during the period from 14 to 25 October 2008.

Our case study (tropical cyclone) appeared over the south of India on 14 and 15 October at 1000 hPa level as an extension of an equatorial trough (Figure 2A,B), and on 16 October it appeared as a low-pressure system over the southwest of India (Figure 1C). At the 700 hPa level, the upper trough associated with the surface low-pressure system became well-defined southwest of India by 16 October, where its associated center (vortex) appeared at (6° N, 65° E) over the Indian Ocean (Figure 2C).

On 17 October the upper trough moved westward and its associated surface cyclonic storm underwent significant strengthening. On 18 October, at the beginning of the increase in strength of the cyclone, the closed 700 hPa contours occurred and moved westward. The higher development in the surface cyclonic storm appeared on 19 October, where its central pressure decreased to 999 hPa (Figure 3). Moreover, a pronounced decrease in the geopotential height at 1000 and 700 hPa levels occurred in association with the deepening surface cyclone. By 20 October, the cyclonic storm moved slowly northwestward and its central geopotential height decreased to less than 20 and 3080 gpm at 1000 and 700 hPa

(Figures 1G and 2G). During the next 24 h, the cyclonic storm also shifted northwestward to reach the coast of south Yemen.

On 21 October the ridge of subtropical high that covers the Arabian Peninsula moved northward, which permitted the cyclone to extend horizontally and move slowly westward. The cyclone moved westward on 22 October and reached the Gulf of Aden, Yemen, and the north of Somalia, which it connected with the developing trough that occurred over the north Red Sea, thus increasing the cyclogenesis over this area. On 23 October the area of the cyclone at the surface decreased and moved slowly eastward to reach the southeast of the Arabian Peninsula and the Arabian sea (Figure 1I,J). While the cyclone at the surface weakened gradually on 22 and 23 October, continuous rainfall occurred over Yemen and southwest of Saudi Arabia due to the interaction between its upper trough with the entrance of the Mediterranean upper trough (Figure 2I,J). The weakening of the cyclone continued on the surface and in the upper air layers, with less instability continuing on 24 and 25 October over southwestern Saudi Arabia and the west of Yemen (Figure 2K,L).

3.2. Vertical Tilt of Tropical Cyclone

It is known that the development of middle-latitude frontal depressions is usually observed with considerable displacements between the circulation centers of the surface and the upper level, and, as the depression strengthens, its centers on the surface and the upper level become vertically tilted. Thus, the displacement in the center of the upper-level vortex from the surface center is defined as the vertical tilt. One of the most important factors controlling both the intensity of TC and tropical cyclogenesis is the environmental vertical wind shear [21–30]. VWS may impede the formation and strengthening of TCs by the entrance of the dry and low entropy air into the initial disturbance of the vortex, and prevent it from deepening by disrupting the formation of a moist column and removing the condensation heat from it [21,31–33].

In this work, we used two techniques to explain the vertical tilt behavior due to the growth in the TC. In the first technique, the cyclone centers were traced on each day at each level and the longitude of the minimum geopotential height (H) values was determined within each center. Figure 4 illustrates the longitudinal displacement of the depression centers with the different vertical pressure levels at 12Z of each day in the period of study (14 to 25 October 2008). It illustrates that during the first day (14 October) a considerable vertical trough (cyclone center) tilt to the west from 1000 to 400 hPa was detected. On the second day (15 October) the tilt of the trough was increased slightly to the west through the levels from 1000 to 500 hPa, but became eastward above 500 hPa. On 17 October, the initial day of the growth period, the vertical westward trough tilt decreased. On 19 and 20 October, the period of the highest cyclone growth, a weak westward trough tilt was detected below 400 hPa, and a further decrease in the westward trough tilt appeared during the last day of the growth period (21 October). On the first day of the decay stage of this cyclone (22 October), the tilt of the trough axis from 1000 to 400 hPa was nearly zero, but in the last two days (24–25 October) the cyclone started filling and the central pressure of the cyclone increased steadily and the tilt became slightly eastward. Generally, the vertical tilt was strongly correlated and affected by the TC intensity changes where, during the growth period, the vertical tilt magnitude increased rapidly, while the TC intensity weakened obviously during the decay period. Moreover, it is clear that the direction of tilt of the TC depends on the intensity of the TC.

When the direction of the tilt was to the west (Figure 4), this led to the strengthening of the cyclone and the increase in circulation, which caused the water vapor to be drawn to a higher level. This contributed to the decrease in total ozone (this is illustrated in Figure 7, particularly on days 19–21 October).

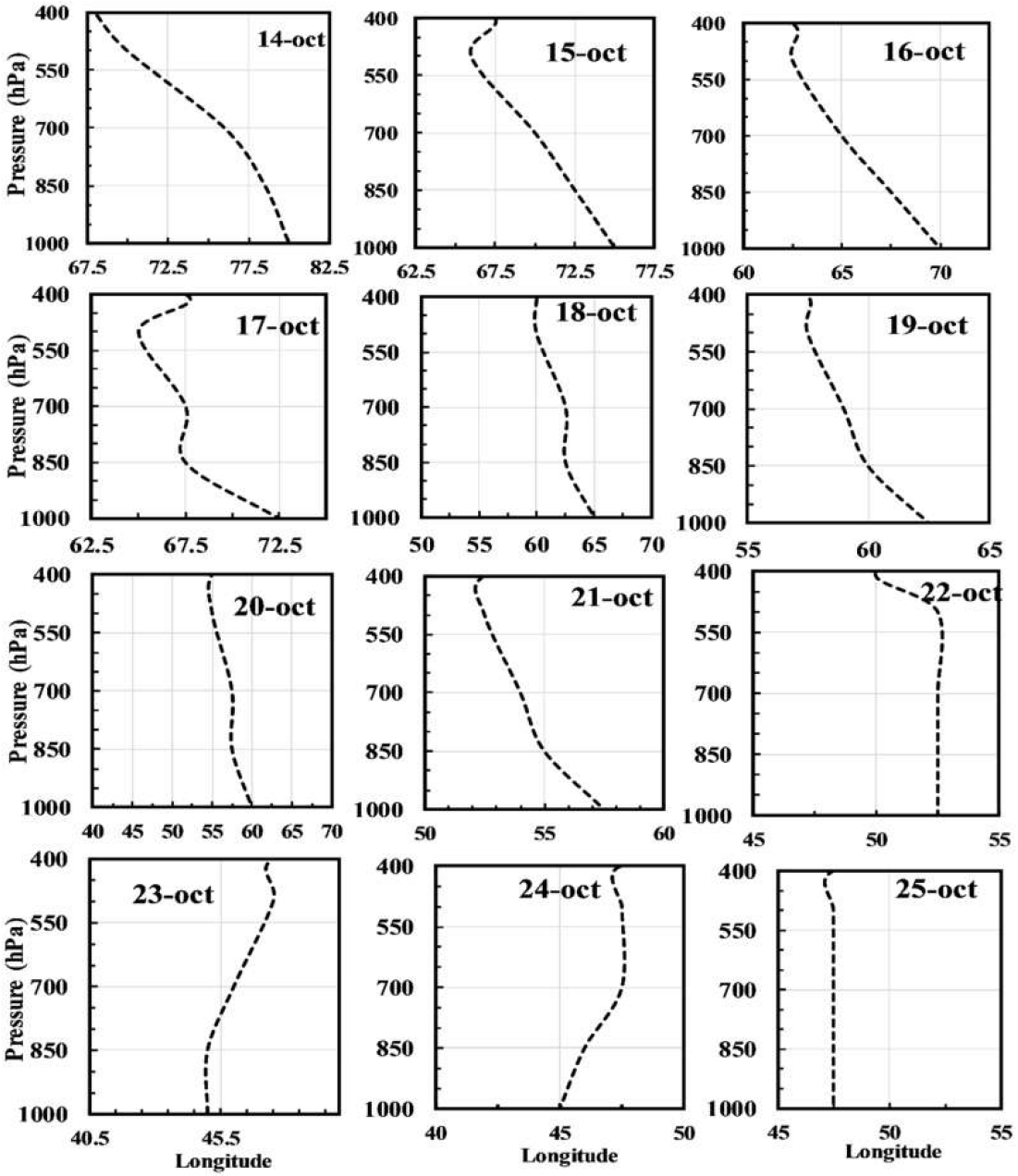

Figure 4. The tilt of geopotential height of the tropical cyclone center from 1000 to 400 hPa at 12Z during the period from 14 to 25 October 2008.

The second technique depends on the value of VWS within two pressure levels from 1000 up to 100 hPa. It was found that the layer between 100 and 1000 hPa has a better representative deep-layer shear effect than the other layers. Moreover, it was found that the layer between 850 (or 700) and 1000 hPa involves the low-layer shear effect and has a higher negative correlation with TC intensity changes than any deep-layer shear through the period of cyclone activity. Figure 5 illustrates the horizontal distribution of the VWS ($\geq$8 m/s) from 1000 to 100 hPa for the period of interest. On 12–14 October, it is clear that the higher values of VWS that appear over the south of India coincided with the surface circulation of our cyclone; its maximum value at the center is more than 16 m/s. With the movement of the cyclone westward, the values of VWS increased and extended horizontally to occupy a large area (55°–90 °E, 10° S–10° N) with a maximum value greater than 24 m/s at (72.5° E, 2.5° N) on 12–15 October. On 12–16 October, the position of higher values at the center of vertical wind shear did not change, while the maximum value increased to become more than 28 m/s. With the beginning of the growth period

(12–17 October), the center of higher values of VWS moved northeastward accompanied by the lower circulation of the cyclone; the maximum value (≥20 m/s) occurred at (67.5° E, 5° N). On 18 and 19 October, the center of the higher values of VWS moved northwestward associated with the movement in the tropical cyclone. In general, the values of VWS decreased during these two days. Another considerable increase in the values of VWS occurred on 20 and 21 October, where the maximum values reached 28 and 24 m/s during the two days, respectively. With the beginning of the decay period (22–25 October), the values of VWS experienced a significant decrease; that is, with the exception of 22 October, the values of VWS were less than 8 m/s during the last three days.

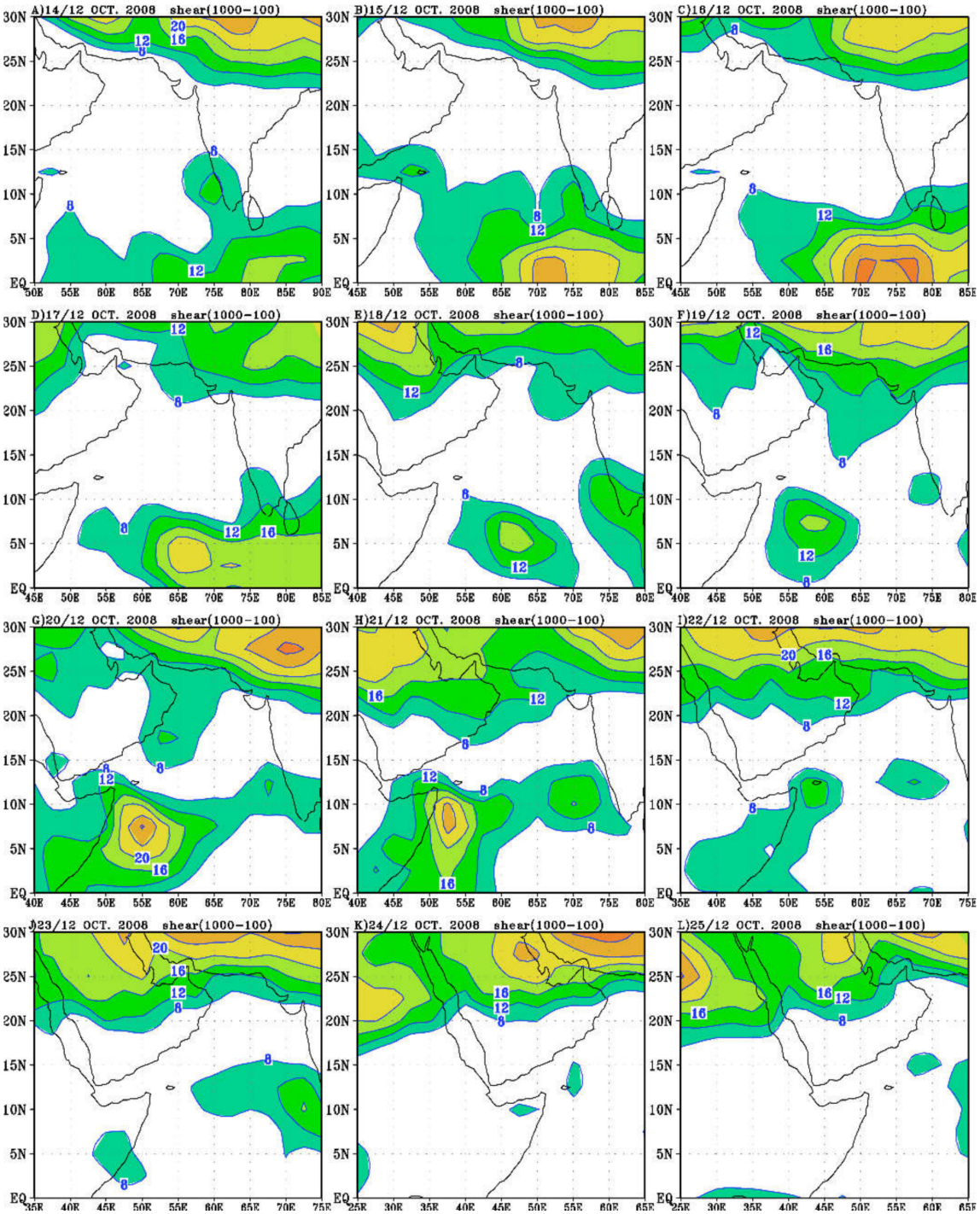

Figure 5. Vertical wind shear values between 1000 and 100 hPa of the tropical cyclone at 12Z during the period from 14–25 October 2008 (**A**–**L**).

3.3. The Horizontal Distribution of TOC

To highlight the relation between TOC and the development of TC, we present here the horizontal distribution of TOC during the period of study. Figure 6 illustrates the horizontal distribution of the evolution of TOC less than 264 DU during the period from 14 to 25 October 2008. Figure 6A displays the values of TCO (≤264 DU) on 12–14 October. It is clear that the lower values of TCO are located over the south of India and the Arabian sea. According to Figure 6B, within 24 h (12–15 October) the low values of TOC propagated slightly eastward associated with the movement in the upper air trough at 700 hPa (Figure 3b) and its magnitude decreased to less than 260 DU. After 24 h (Figure 6D), the values of TOC decreased (≤260 DU) and the area of lower values of TOC extended to cover the northeast of the Pacific in association with the formation of the cut-off low at 700 hPa (Figure 3b). On 12–18 October, the center of the cyclone at 700 hPa was located at (62.5° E, 6° N) where the lowest values of TOC appeared over, and north-northeast of, the area containing the cyclone circulation (Figure 6E). This situation was continued until 12–21 October, where the main core of lower values of TOC was associated and located over, and north-northeast of, the area of the 700 hPa low-pressure center (Figure 6F,H). By 12–22 October (Figure 6I), it is interesting to note that the area of lowest values of TOC decreased where the cyclone began to weaken and moved slowly eastward. On 24 and 25 October, the cyclone was located over the south Red Sea, and it can be noted that the values of TOC increased (Figure 6K,L). Finally, we can conclude there is a positive correlation between the development (deepening) of a tropical cyclone with the decrease in TOC, where the lower values of TCO occurred during the growth period of our cyclone.

3.4. TOC Variation during Tropical Cyclone

In this section, we examine the variation in TOC over the inner domain containing the TC through October 2008. This domain changed with time to contain our cyclone during its life cycle (Figure 2), and so the average of the TOC and the selected meteorological parameters were calculated only across this domain to provide a better view and investigation of the total amount of ozone variation with meteorological parameters. Figure 7 illustrates the daily values of TOC at the points (7° N, 62° E), (5° N, 60° E), (9° N, 60° E), and (12° N, 55° E) during October 2008. These four points represent the position of the cyclone center on the days 18, 19, 20, and 21 October, respectively. It is clear that the values of TOC on each of these four days are less than the corresponding monthly average at this point. It was found that the value of total ozone on 18 October (261.2 DU) was less than the monthly average by 8 DU, whereas on 19 October the value of TOC was less than the monthly average by 7 DU. On 20 October, the average monthly value of TOC at the center cyclone point (9° N, 60° E) was 268.5 DU, which is greater than the daily values by 12 DU. Moreover, the values of TOC at the center of the cyclone on 21 October were less than the average (267.6 DU) by 8 DU.

Before the development of the TC, there was a greater increase in the trend of TOC, whereas during and after the development of the TC, the TOC was mostly reduced, as illustrated in Figure 7. The sudden drop in the concentration of TOC was detected at the maximum intensity of the TC occurrence, which appeared on 20 October. These results are consistent with Nerushev [34] and Singh and Nair [11] for severe and very severe TCs.

Figure 8 shows the anomalies (the difference between the daily and the monthly values) of TOC at the tropical cyclone's center during the period of study. It is clear that all the anomalies were negative during the period of cyclone development with a maximum negative value on 20 October (−10 DU). The ozone anomalies (Figure 8) vary according to the cyclonic system, and the strength of the TC affects their amount. Therefore the relationship between the strength of the TC and the greatest decrease in TOC is anticipated at a specific region.

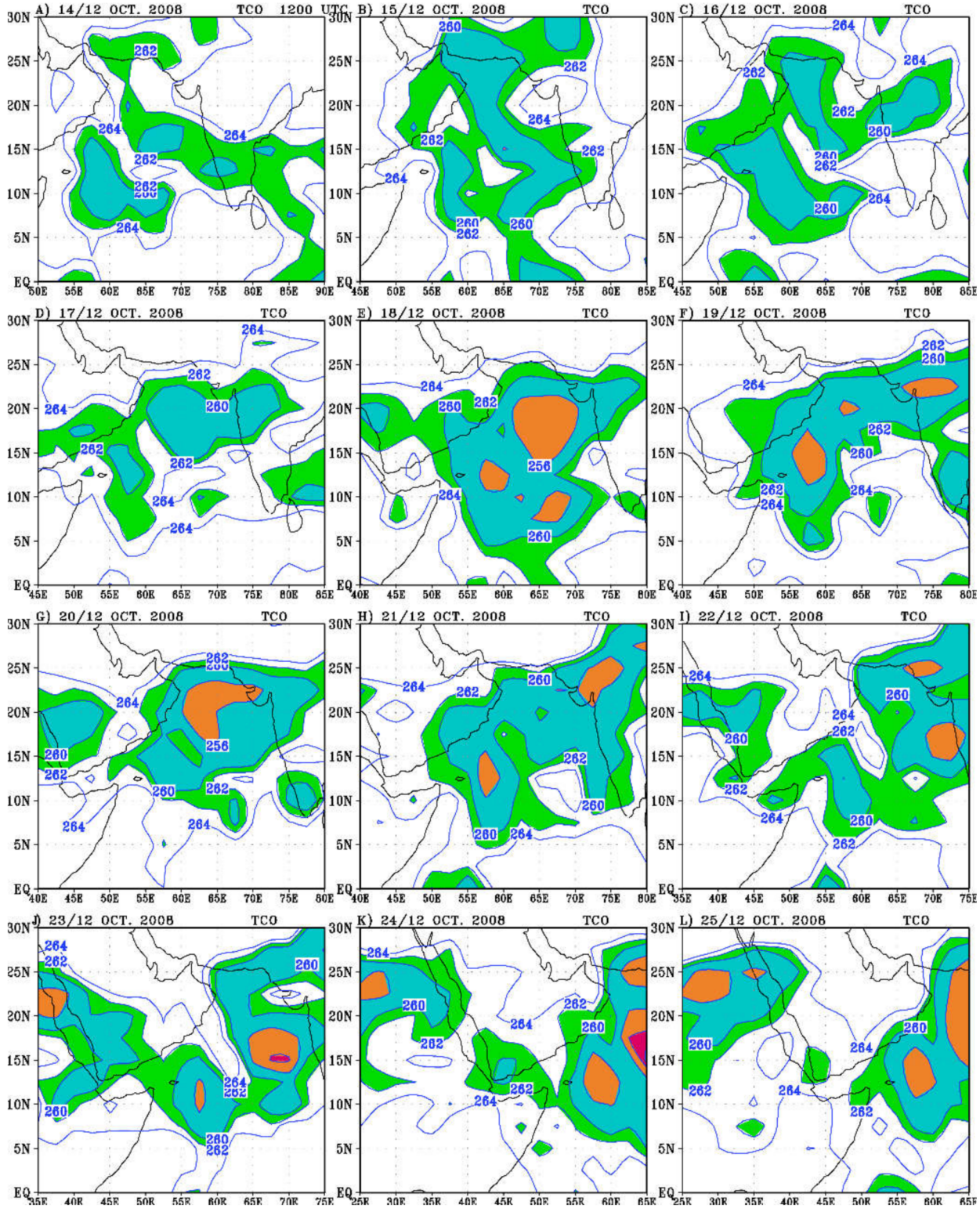

Figure 6. The horizontal distribution of the vertically integrated values of total ozone (≤264 DU) at 12Z during the period from 14 to 25 October 2008 (**A**–**L**).

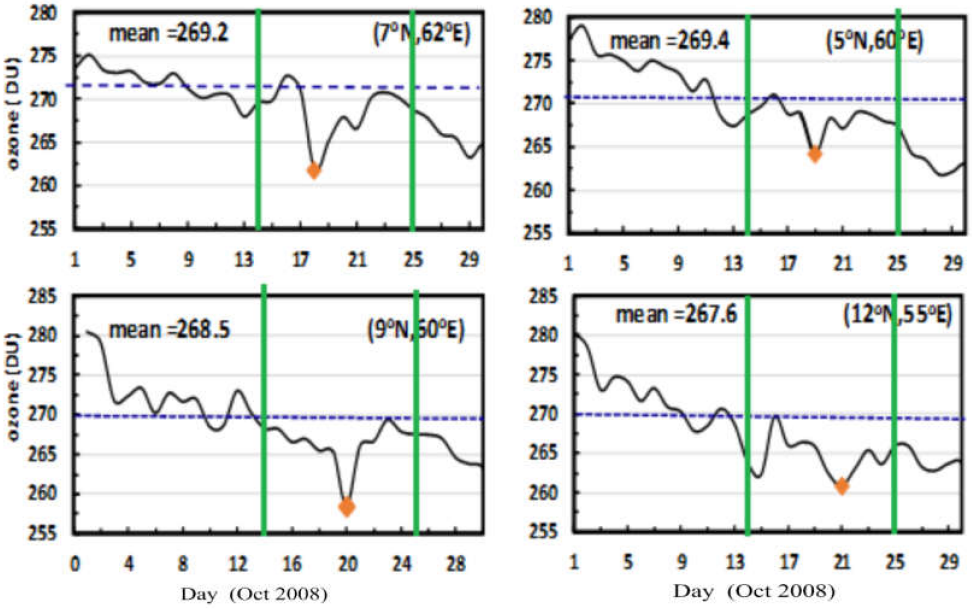

Figure 7. Daily total column ozone at the points (7° N, 62° E), (5° N, 60° E), (9° N, 60° E), and (12° N, 55° E) during the month October 2008.

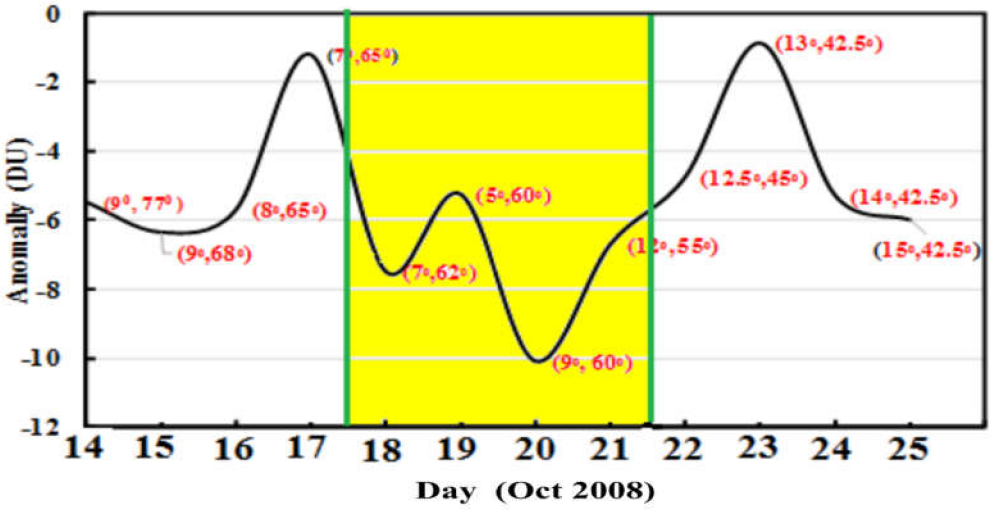

Figure 8. The anomalies (the difference between the daily and the monthly values) of TOC at the tropical cyclone center during the period of study.

Percentage variations between the daily mean (O_3D) and monthly mean (O_3M) TOC in the inner domain around the TC center at its development were studied computed as $((O_3D - O_3M) \times 100/O_3D)$, where O_3M is the average of TOC during the period from 1 to 31 October 2008. Percentage daily variation of TOC (closest to the cyclone center) was calculated during the period from 14 to 25 October 2008 (Figure 9). Generally, it is clear that the values of the percentage daily variation of TOC were negative for all of the days of our study. In addition, it was found that the percentage daily variation in TOC varied from day to day according to the intensity of the tropical cyclone, where its maximum value, of −4.1%, occurred on 20 October, whereas the minimum value (−1.5%) occurred on 17 October.

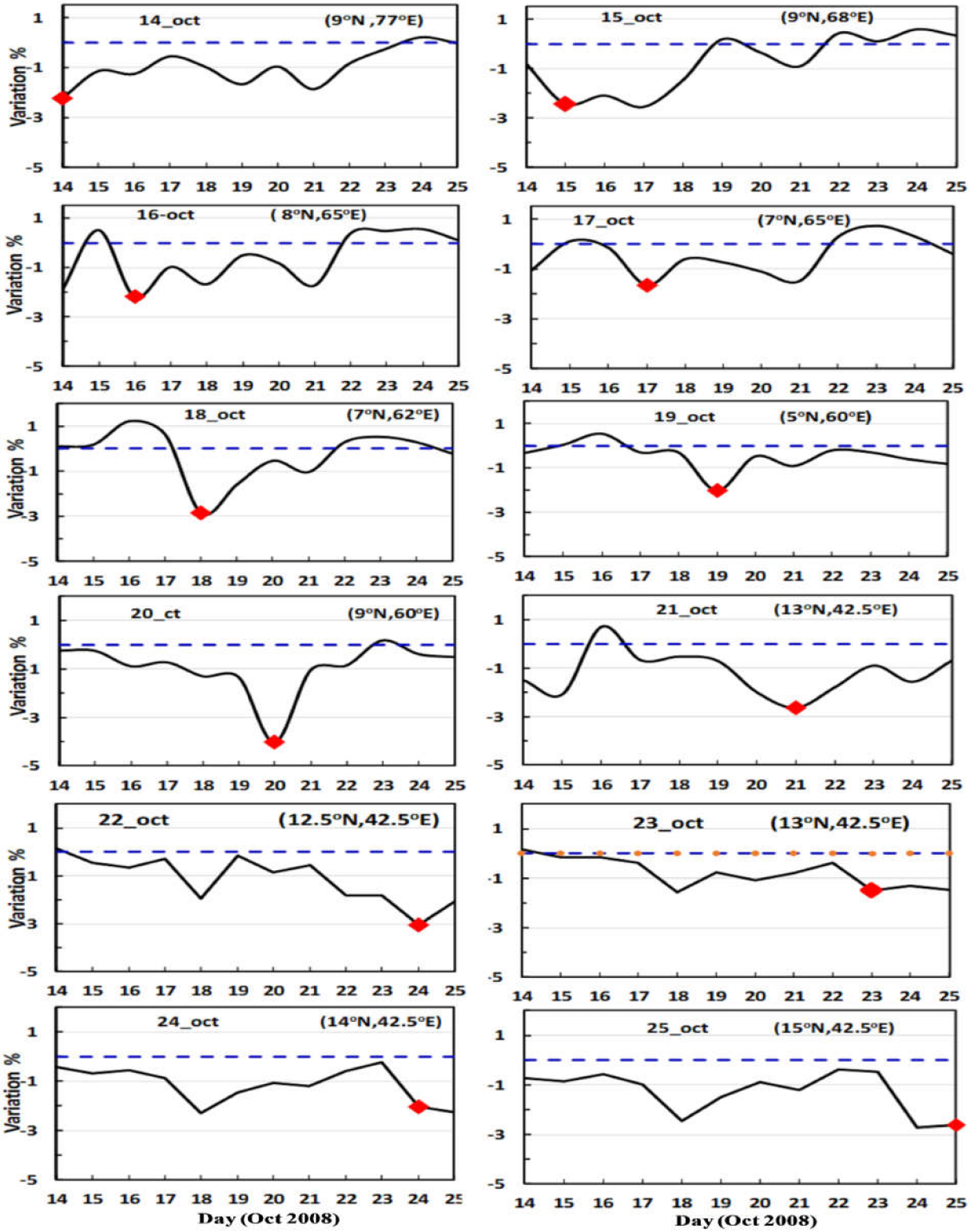

Figure 9. Percentage variation in the daily total column ozone from the monthly mean at each point on the tropical cyclone track from 14 to 25 October 2008.

3.5. Time Height Variations of Ozone Mass Mixing Ratio

Figure 10 illustrates the time height variations of OMR during the period of study, where Figure 10a presents the values of OMR at the cyclone center between the levels of 100 to 1 hPa during the period of study, and Figure 10b shows the values of OMR at the center of the cyclone from level 1000 to 125 hPa during the period of study. It is

clear that the higher values of OMR appear between 20 and 3 hPa with maximum values (>1600 ppm) between 10 and 7 hPa. The values of OMR decreased gradually above and below this layer (11–6 hPa); its values reached about 500 ppm at 1 hPa and also at 45 hPa. The maximum gradient of OMR appeared between 500 and 12 hPa and between 5 and 1 hPa. The gradient of OMR decreased between 100 and 50 hPa. Below 100 hPa, the values of OMR are considered very small compared to the upper values (those above 100 hPa). It is clear that the effect of tropical cyclones appears below 100 hPa (around the tropopause). Figure 10b shows the time height variations in OMR at the center from the 1000 to 125 hPa level. On 14 October, the values of OMR increased gradually from the surface up to 150 hPa. A pronounced increase (>9 ppm) in OMR occurred from 900 to 550 hPa during the period 15 to 19 October and also from 21 to 25 October. On 21 October, the values of OMR increased from the surface to 550 hPa. A noticeable decline in OMR appeared between 550 and 200 hPa during most days.

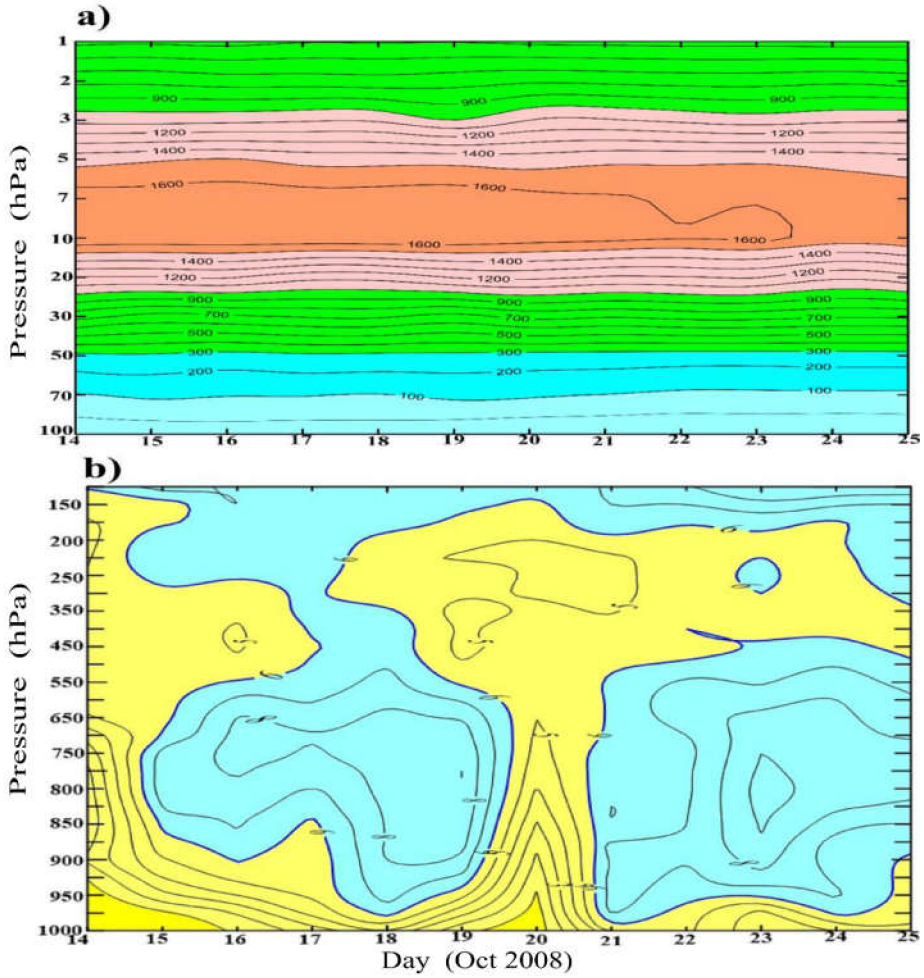

Figure 10. Vertical profile of ozone mass mixing ratio (ppm) at 37 levels (**a**) from 100 to 1 hPa and (**b**) from 1000 to 100 hPa during tropical cyclone event days from 14 to 25 October 2008.

Figure 11 illustrates the horizontal distribution of relative humidity (≥40%) at 700 hPa throughout the period of study, and Figure 12 shows the time height variation of the average relative humidity (1000–70 hPa) in the domain enclosing the tropical cyclone during the period of study. Figure 13 illustrates the time height variation of vertical motion (ω) at the levels from 1000 to 1 hPa in the domain enclosing the tropical cyclone during the same period. Generally, it is clear that a huge amount of water vapor amount advected vertically to the upper levels due to the strong upward motion during the pre-storm and growth periods (14 to 21 October). The maximum values of upward motion ($-\omega$) occurred during the period from 15 and 18 October (especially between the 650–150 hPa levels) and

worked to lift large amounts of water vapor to the upper atmosphere, where we found that the values of relative humidity of 100% reached to and above 100 hPa during the period from 14 to 21 October. Above 900 hPa during the decay period, the downward motion (+ω) dominates at most levels, in association with a large decrease in the relative humidity at all levels.

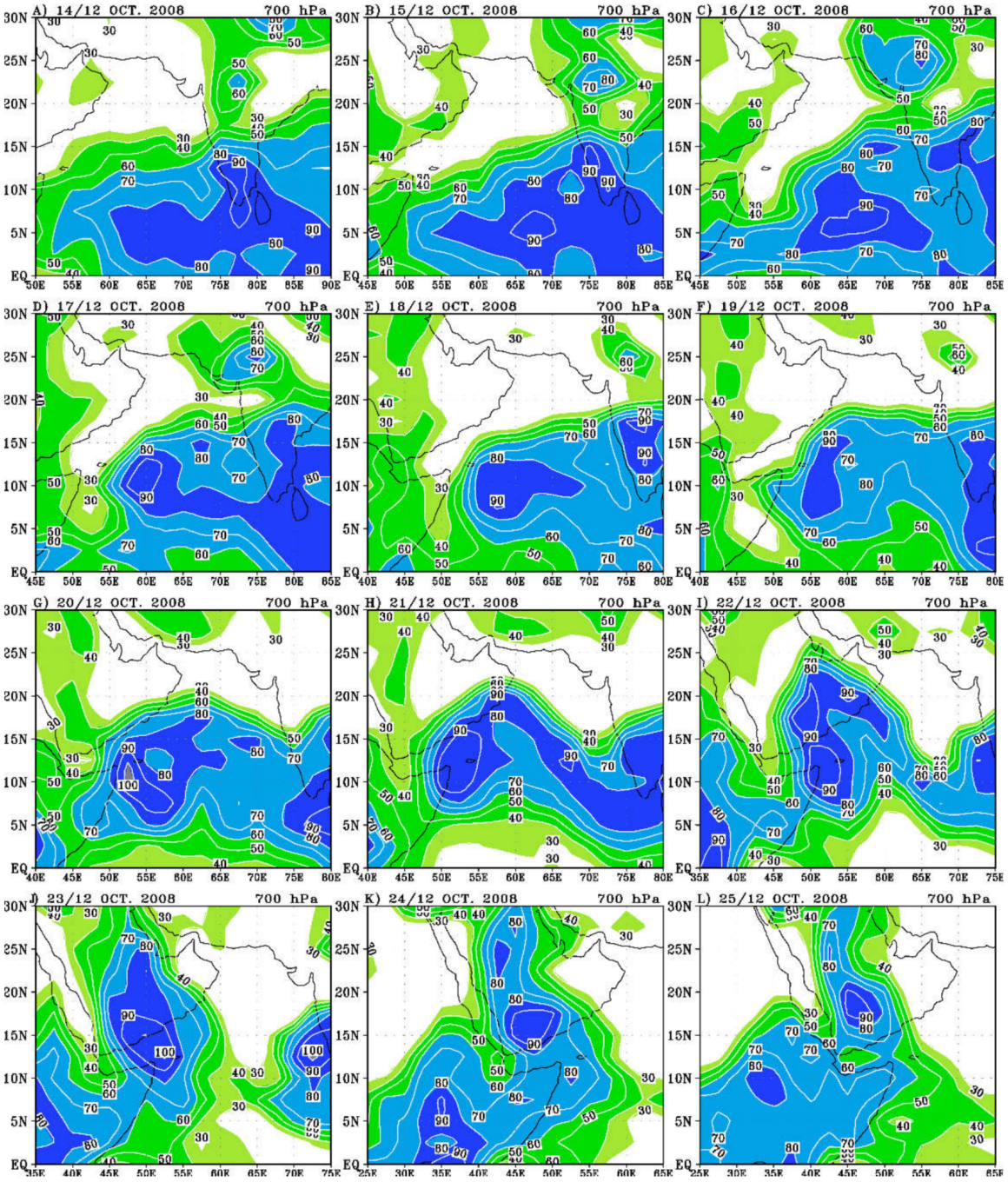

Figure 11. The horizontal distribution of relative humidity (≥40%) at 12Z during the period from 14 to 25 October 2008 (**A**–**L**).

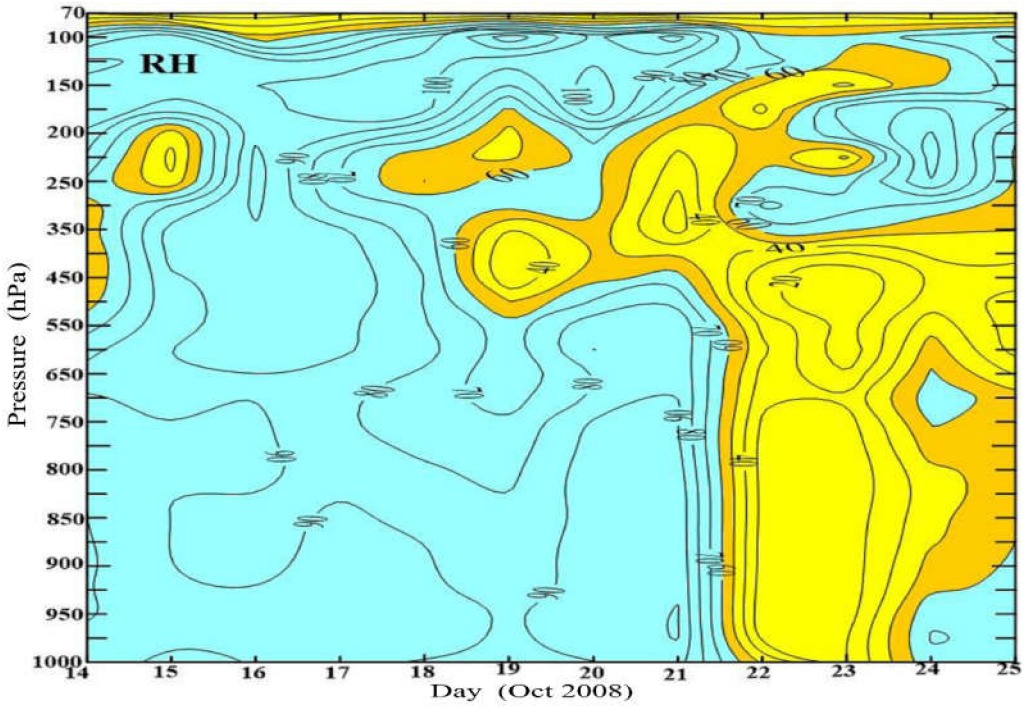

Figure 12. Vertical profile of relative humidity (1000–70 hPa) during tropical cyclone event days from 14 to 25 October 2008.

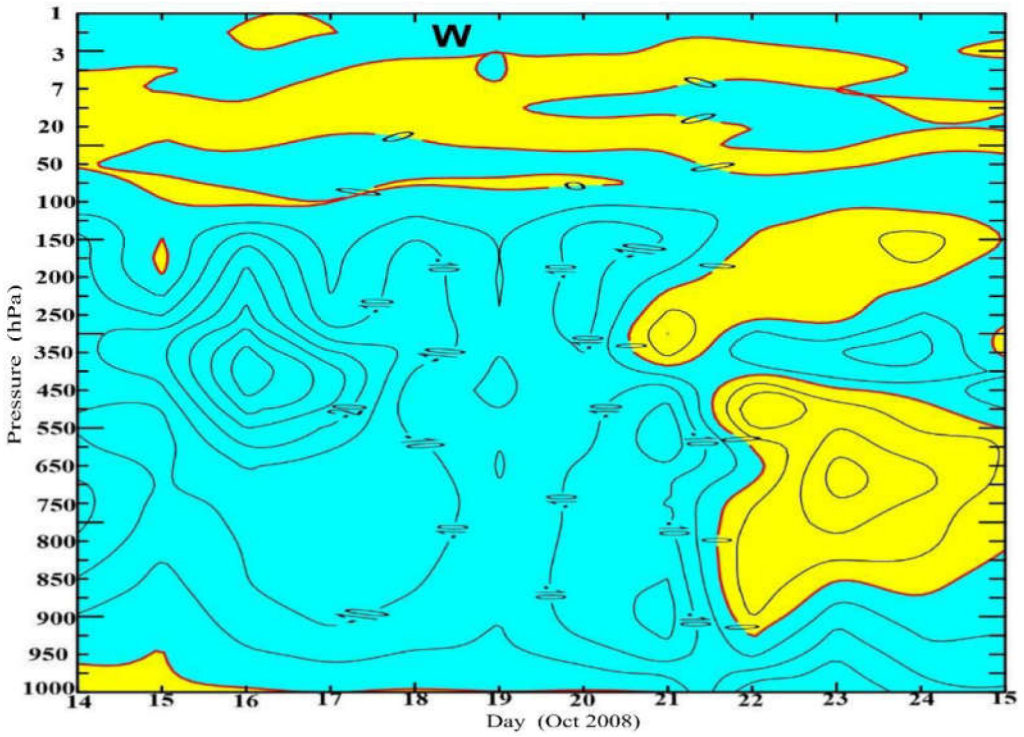

Figure 13. Vertical profile of upward motion (W) at the levels of 1000–1 hPa during the period of study.

The lowest value of TOC throughout our TC, as shown in Figures 6 and 8, occurred because of the oversized amount of water vapor injected from the troposphere into the stratosphere during the deep convection process (Figure 12). This injected water vapor is photo dissociated into hydroxide (OH) and oxygen atomic (O) by the highest solar radiation received within the stratosphere layer resulting in more stratospheric ozone

depletion. Moreover, the percentage of the tropospheric ozone formation is reduced under the cloud level, whereas the ozone decay rate above the cloud level is enhanced due to the cloud backscattering. Furthermore, the upward transport of ozone-poor air from the troposphere gradually changes the ozone-rich air in the stratosphere previously and through the TC. Continuous decrease in TOC over the locations of the cyclone tracks shown in Figures 6 and 8 was observed because of the increase in the stratospheric outflow of ozone-rich air and the inflow of ozone poor-air due to the increase in surface wind speed and the decrease in pressures.

TCs may play a serious role in the amount of water vapor injected into the stratosphere, as shown in Figure 12. Therefore, the TCs can play a crucial role in determining the mixed ratio of water vapor in the stratosphere. The tropopause is cooler than both the troposphere and stratosphere, and represents a barrier to water vapor lifting into the stratosphere. As a result, once the air enters the tropopause it becomes extremely cold, causing almost all of the water vapor to freeze and then fall. Moreover, the current of the very deep cloud associated with the TCs can penetrate the tropopause, and the ice drops into the warmer stratosphere, where it eventually evaporates. Singh and Singh [35] pointed out that the transportation of water vapor into the stratosphere from the troposphere can occur through shifting air currents. Bates and Nicolet [36] stated that the water vapor in the stratosphere becomes photo-dissociated to radical OH as follows:

$$H_2O + h\upsilon \rightarrow OH + H$$

$$OH + h\upsilon \rightarrow O + H$$

$$O + O + M \rightarrow O_2 + M$$

where the third body (M) saves the energy of reaction and momentum. The OH radical is also produced by photodissociation of nitrous and nitric acid in the troposphere and lower stratosphere as follows:

$$HONO + h\upsilon \rightarrow OH + NO$$

$$HNO_3 + h\upsilon \rightarrow OH + NO_2$$

Ozone can be depleted by the OH radical and atomic O with the catalytic cycle as follows:

$$OH + O_3 \rightarrow HO_2 + O_2$$

$$HO_2 + O \rightarrow OH + O_2$$

The formed NO will join with available oxygen and produce NO_2; hence, it may be removed in the form of acid rain from the atmosphere during the TC. TCs that start in the Indian Ocean bring a large amount of water vapor from the Indian and Arabian Oceans and take away most of the pollutants from the troposphere through various precipitation processes, which lead to the formation of tropospheric ozone. The huge presence of clouds allows a smaller amount of solar radiation to enter the troposphere, and makes a small contribution to the formation of tropospheric ozone, which resulted in a sharp drop in tropospheric ozone density during the studied TC.

4. Conclusions

This paper aimed to study the variation in TOC over the northwest Indian Ocean during the life cycle of the tropical cyclone that occurred throughout the period 14 to 25 October 2008. The characteristics of tropical cyclone tilts, with vertically varying background flows, were also inspected preliminarily in the current study. The vertical wind shear was estimated to be one of the most important dynamical parameters of the large-scale environment related to TC formation, structure, and intensity changes. It was found that the magnitude of the VWS increased during the growth period, whereas VWS weakened during the decay period. Anomalies of daily TOC were found to steadily reduce before and during the cyclone formation, followed by an increasing trend after the dissi-

pation of the cyclone. A sharp drop in TOC exceeded 11 DU as shown at the maximum intensity of the TC, which was characterized by the highest wind speed in the regions where the TC was intensifying. In the growth period of the TC, the outflow occurred and developed in the upper levels accompanied by the maximum vertical velocities, and was extended beyond the tropopause and into the lower stratosphere. As a result of the removal of ozone due to the developed outflow, the TOC decreased. The observed variation in TOC follows the present dynamical and chemical concepts for the ozone depletion process. The lowest value of TOC throughout the studied TC occurred due to the huge amount of injected water vapor from the troposphere into the stratosphere through the convection processes. This injected water vapor is mostly photo dissociated into radical OH and atomic oxygen by the highest solar radiation in the lower and upper stratosphere, which leads to a significant decline in ozone in the stratosphere. Additionally, under the cloud level, the rate of tropospheric ozone formation decreases, whereas above that level, the cloud increases the rate of ozone depletion due to backscattering. In addition, the upward transport of ozone-poor air from the troposphere is gradually replaced by the ozone-rich air in the stratosphere before and during the TC.

Author Contributions: Conceptualization, S.A.-K., M.A.-M., H.A.B. and A.A.; Data curation, M.A.-M., A.A. and A.B.; Formal analysis, M.A.-M. and H.A.B.; Funding acquisition, S.A.-K.; Methodology, S.A.-K., M.A.-M., H.A.B., M.M. and A.B.; Project administration, S.A.-K.; Resources, M.A.-M.; Software, A.A. and A.B.; Supervision, S.A.-K., M.A.-M. and H.A.B.; Validation, A.A and M.M.; Visualization, A.A. and A.B.; Writing–original draft, M.M.; Writing–review & editing, H.A.B. All authors have read and agreed to the published version of the manuscript.

Funding: This research was funded by Deanship of Scientific Research at Princess Nourah Bint Abdulrahman University, through the Research Funding program (Grant No. FRP-1442-21).

Institutional Review Board Statement: Not applicable.

Informed Consent Statement: Not applicable.

Data Availability Statement: The data supporting the findings of this article are included within the article and were obtained from https://apps.ecmwf.int/datasets/data/interim-full-daily/levtype=sfc/ (accessed on 23 March 2020) for TCO and https://apps.ecmwf.int/datasets/data/interim-full-daily/levtype=pl (accessed on 23 March 2020) for OMR.

Acknowledgments: The researchers express their great thanks and appreciation to the Higher Studies and Scientific Research Agency at the University of Princess Nourah Bint Abdulrahman for their support of research project No. (FRP-1442-21) and thank the Princess Nora bint Ab-dulrahman University for providing all the facilities to work in this research, and to all those who contributed to this study.

Conflicts of Interest: All authors declare that they have no any conflict of interest.

References

1. Baray, J.-L.; Randriambelo, T.; Baldy, S.; Ancellet, G. Tropical cyclone Marlene and stratosphere-troposphere exchange. *J. Geophys. Res. Spa. Phys.* **1999**, *104*, 13953–13970. [CrossRef]
2. Ratnam, M.V.; Babu, S.R.; Das, S.S.; Basha, G.; Krishnamurthy, B.V.; Venkateswararao, B. Effect of tropical cyclones on the stratosphere–troposphere exchange observed using satellite observations over the north Indian Ocean. *Atmos. Chem. Phys. Discuss.* **2016**, *16*, 8581–8591. [CrossRef]
3. Das, S.S. A new perspective on MST radar observations of stratospheric intrusions into-troposphere associated with tropical cyclone. *Geophys. Res. Lett.* **2009**, *36*. [CrossRef]
4. Li, D.; Vogel, B.; Müller, R.; Bian, J.; Günther, G.; Li, Q.; Zhang, J.; Bai, Z.; Vömel, H.; Riese, M. High tropospheric ozone in Lhasa within the Asian summer monsoon anticyclone in 2013: Influence of convective transport and stratospheric intrusions. *Atmos. Chem. Phys. Discuss.* **2018**, *18*, 17979–17994. [CrossRef]
5. Pan, L.L.; Homeyer, C.R.; Honomichl, S.; Ridley, B.A.; Weisman, M.; Barth, M.C.; Hair, J.W.; Fenn, M.A.; Butler, C.; Diskin, G.S.; et al. Thunderstorms enhance tropospheric ozone by wrapping and shedding stratospheric air. *Geophys. Res. Lett.* **2014**, *41*, 7785–7790. [CrossRef]
6. Bian, J.; Li, D.; Bai, Z.; Li, Q.; Lyu, D.; Zhou, X. Transport of Asian surface pollutants to the global stratosphere from the Ti-betan Plateau region during the Asian summer monsoon. *Natl. Sci. Rev.* **2020**, *7*, 516–533. [CrossRef]

7. Danielsen, E.F. In situ evidence of rapid, vertical, irreversible transport of lower tropospheric air into the lower tropical stratosphere by convective cloud turrets and by larger-scale upwelling in tropical cyclones. *J. Geophys. Res. Sp. Phys.* **1993**, *98*, 8665–8681. [CrossRef]
8. Das, S.S.; Uma, K.N.; Bineesha, V.N.; Suneeth, K.V.; Ramkumar, G. Four-decadal climatological intercomparison of rocketsonde and radiosonde with different reanalysis data: Results from Thumba Equatorial Station. *Q. J. R. Meteorol. Soc.* **2016**, *142*, 91–101. [CrossRef]
9. Pan, L.L.; Honomichl, S.B.; Randel, W.J.; Apel, E.C.; Atlas, E.L.; Beaton, S.P.; Bresch, J.F.; Hornbrook, R.; Kinnison, D.E.; Lamarque, J.; et al. Bimodal distribution of free tropospheric ozone over the tropical western Pacific revealed by airborne observations. *Geophys. Res. Lett.* **2015**, *42*, 7844–7851. [CrossRef]
10. Randel, W.J.; Park, M. Deep convective influence on the Asian summer monsoon anticyclone and associated tracer variabil-ity observed with Atmospheric Infrared Sounder (AIRS). *J. Geophys. Res. Atmos.* **2006**, *111*. [CrossRef]
11. Singh, D.; Nair, S. Total ozone depletion due to tropical cyclones over Indian Ocean. In Proceedings of the International TOVS study Conference, Angra dos Reis, Brazil, 7–13 May 2008.
12. Midya, S.K.; Dey, S.S.; Chakraborty, B. Variation of the total ozone column during tropical cyclones over the Bay of Bengal and the Arabian Sea. *Theor. Appl. Clim.* **2012**, *117*, 63–71. [CrossRef]
13. Heymsfield, G.M.; Simpson, J.; Halverson, J.; Tian, L.; Ritchie, E.; Molinari, J. Structure of Highly Sheared Tropical Storm Chantal during CAMEX-4. *J. Atmos. Sci.* **2006**, *63*, 268–287. [CrossRef]
14. Li, Q.; Duan, Y.; Yu, H.; Fu, G. A High-Resolution Simulation of Typhoon Rananim (2004) with MM5. Part I: Model Verification, Inner-Core Shear, and Asymmetric Convection. *Mon. Weather. Rev.* **2008**, *136*, 2488–2506. [CrossRef]
15. Reasor, P.D.; Rogers, R.; Lorsolo, S. Environmental flow impacts on tropical cyclone structure diagnosed from airborne Doppler radar composites. *Mon. Weather. Rev.* **2013**, *141*, 2949–2969. [CrossRef]
16. Xu, Y.; Wang, Y. On the Initial Development of Asymmetric Vertical Motion and Horizontal Relative Flow in a Mature Tropical Cyclone Embedded in Environmental Vertical Shear. *J. Atmos. Sci.* **2013**, *70*, 3471–3491. [CrossRef]
17. Barnes, C.E.; Barnes, G.M. Eye and Eyewall Traits as Determined with the NOAA WP-3D Lower-Fuselage Radar. *Mon. Weather. Rev.* **2014**, *142*, 3393–3417. [CrossRef]
18. DeHart, J.C.; Houze, R.A.; Rogers, R.F. Quadrant distribution of tropical cyclone inner-core kinematics in relation to environmental shear. *J. Atmos. Sci.* **2014**, *71*, 2713–2732. [CrossRef]
19. Li, Q.; Wang, Y.; Duan, Y. A Numerical Study of Outer Rainband Formation in a Sheared Tropical Cyclone. *J. Atmos. Sci.* **2017**, *74*, 203–227. [CrossRef]
20. Dee, D.P.; Uppala, S.M.; Simmons, A.J.; Berrisford, P.; Poli, P.; Kobayashi, S.; Andrae, U.; Balmaseda, M.A.; Balsamo, G.; Bauer, D.P.; et al. The ERA-Interim reanalysis: Configuration and performance of the data assimilation system. *Q. J. R. Meteorol. Soc.* **2011**, *137*, 553–597. [CrossRef]
21. Gray, W.M. Global view of the origin of tropical disturbances and storms. *Mon. Weather Rev.* **1968**, *96*, 669–700. [CrossRef]
22. McBride, J.L.; Zehr, R. Observational Analysis of Tropical Cyclone Formation. Part II: Comparison of Non-Developing versus Developing Systems. *J. Atmos. Sci.* **1981**, *38*, 1132–1151. [CrossRef]
23. Merrill, R.T. Environmental Influences on Hurricane Intensification. *J. Atmos. Sci.* **1988**, *45*, 1678–1687. [CrossRef]
24. DeMaria, M. The effect of vertical shear on tropical cyclone intensity change. *J. Atmos. Sci.* **1996**, *53*, 2076–2088. [CrossRef]
25. Wang, Y.Q.; Wu, C.C. Current understanding of tropical cyclone structure and intensity changes–A review. *Meteorol. Atmos. Phys.* **2004**, *87*, 257–278. [CrossRef]
26. Paterson, L.A.; Hanstrum, B.N.; Davidson, N.E.; Weber, H.C. Influence of environmental vertical wind shear on the inten-sity of hurricane-strength tropical cyclones in the Australian region. *Mon. Weather Rev.* **2005**, *133*, 3644–3660. [CrossRef]
27. Zeng, Z.; Wang, Y.; Wu, C.-C. Environmental Dynamical Control of Tropical Cyclone Intensity—An Observational Study. *Mon. Weather. Rev.* **2007**, *135*, 38–59. [CrossRef]
28. Zeng, Z.; Chen, L.; Wang, Y. An Observational Study of Environmental Dynamical Control of Tropical Cyclone Intensity in the Atlantic. *Mon. Weather. Rev.* **2008**, *136*, 3307–3322. [CrossRef]
29. Zeng, Z.; Wang, Y.; Chen, L. A statistical analysis of vertical shear effect on tropical cyclone intensity change in the North Atlantic. *Geophys. Res. Lett.* **2010**, *37*. [CrossRef]
30. Wang, Y.; Rao, Y.; Tan, Z.-M.; Schönemann, D. A Statistical Analysis of the Effects of Vertical Wind Shear on Tropical Cyclone Intensity Change over the Western North Pacific. *Mon. Weather. Rev.* **2015**, *143*, 3434–3453. [CrossRef]
31. Emanuel, K.A. The Finite-Amplitude Nature of Tropical Cyclogenesis. *J. Atmos. Sci.* **1989**, *46*, 3431–3456. [CrossRef]
32. Bister, M.; Emanuel, K.A. The Genesis of Hurricane Guillermo: TEXMEX Analyses and a Modeling Study. *Mon. Weather Rev.* **1997**, *125*, 2662–2682. [CrossRef]
33. Nolan, D.S. For tropical cyclogenesis? *Australian Meteorological Magazine*, 2007, pp. 241–246.
34. Nerushev, A.F. Perturbations of the ozone layer induced by intense atmospheric vortices. *Int. J. Remote. Sens.* **2008**, *29*, 2705–2732. [CrossRef]
35. Singh, D.; Singh, V. Impact of tropical cyclone on total ozone measured by TOMS–EP over the Indian region. *Curr. Sci.* **2007**, *93*, 471–476.
36. Bates, D.R.; Nicolet, M. The photochemistry of atmospheric water vapor. *J. Geophys. Res. Sp. Phys.* **1950**, *55*, 301–327. [CrossRef]